Chapter 5

Surface Ruptures of the M_w 6.8 March 2011 Tarlay Earthquake, Eastern Myanmar

Soe Thura Tun[1], Yu Wang[2, 3], Saw Ngwe Khaing[4], Myo Thant[5], Nyunt Htay[6], Yin Myo Min Htwe[7], Than Myint[1] and Kerry Sieh[3]

1. Myanmar Earthquake Committee, Myanmar Engineering Society, Hlaing University's campus, Yangon, Myanmar
2. Division of Geological and Planetary science, California Institute of Technology, Pasadena, CA 91125, USA
3. Earth Observatory of Singapore, Nanyang Technological University?N2-01A-10B, 50 Nanyang Avenue, Singapore 639798
4. Department of Geology, Hinthada University, Hinthada, Ayeyarwady, Myanmar
5. Department of Geology, University of Yangon, Yangon, Myanmar
6. Myanmar Geosciences Society, Hlaing Universities' campus, Yangon, Myanmar
7. Department of Meteorology and Hydrology, Office building No-5, Ministry of Transport, Naypyidaw, Myanmar

Abstract

Field observations indicate that the M_w 6.8 Tarlay (Myanmar) earthquake on 24 March 2011 resulted from the rupture of a short section of the left-lateral Nam Ma Fault. The Nam Ma Fault is one of many left-lateral faults that comprise the Shan fault system, which has accommodated more than 100 km left-lateral displacement in a triangular area between the Red River Fault and the Sagaing Fault around the eastern Himalayan syntaxis. We document coseismic left-lateral offsets ranging from approximately 10 cm to more than 1.25 m over a 19-km section of the fault from the field investigation and the interpretation of high-resolution satellite imagery. The comparison of the field survey results and the interpretation from the satellite imagery suggests that most of the

offset paddy-related features faded out within one to two years except for those in a few areas at the western part of the fault. Our field measurements also indicate that the magnitude of sinistral offset decreases gradually eastward before terminating inside the Tarlay Basin, along the southern edge of a 2-km-wide releasing stepover.

Our survey confirms that a structurally limited segment of the westernmost part of the Nam Ma Fault was responsible for the Tarlay earthquake. If the rest of the Nam Ma fault moves entirely in a single event, it is capable of generating an M_w 7.7 earthquake between Myanmar and Laos.

Introduction

Myanmar spans a very complex and broad tectonic belt that accommodates the northward translation of the Indian Plate past the Sunda Plate (e.g., Socquet et al., 2006). This motion is primarily expressed by right-lateral slip on the Sagaing Fault, which bisects Myanmar from south to north (Fig.1) (Win Swe, 1970; Curray et al., 1979; Le Dain et al., 1984), and right-lateral oblique convergence across the northern Sunda megathrust beneath the western coast and adjacent Indoburman Ranges (Nielsen et al., 2004; Socquet et al., 2006).

To the east, Myanmar also experiences the tectonic effects of the southward extrusion of southern China around the eastern end of the Himalayan collision zone (e.g., Le Dain et al., 1984; Holt et al., 1991; Lacassin et al., 1998; Wang et al., 1998). This manifests itself as a set of arcuate, predominately left-lateral, southwest-striking faults called the Shan fault system that span the border of China with Vietnam, Laos, Thailand and Myanmar (Fig. 1). The Shan fault system, including the Nanting Fault, the Jing Hong fault, Mengxing Fault, the Nam Ma Fault, the Mae Chan Fault and other parallel left-lateral faults have accommodated more than 100 km of left-lateral displacement at the northern Sunda plate between the Burma and the Southern China plate (Wang et al., in preparation). Together with their conjugate right-lateral faults, this fault system plays an important role in accommodating the deformation around the eastern Himalayan syntaxis, predominantly from China toward Myanmar (e.g., Holt et al., 1991; Wang et al., 1998; Socquet and Pubellier, 2005).

In the past century, the Shan fault system has experienced many significant and destructive earthquakes, including the 1976 Longling earthquake (M_w 6.7), the 1988 Lancang earthquake (M_w 7.0) and the 1995 Menglian earthquake (M_w 6.8) (Fig.1). Although their focal mechanisms and locations are consistent with the geometries of the conjugate right-lateral and left-lateral faults within the Shan fault system, very few surface ruptures associated these events have been documented. Thus, the source of earthquakes and the rupture behaviors of these strike-slip faults remain largely unclear.

The Nam Ma fault is one of these left-lateral faults for which knowledge was very limited. The 215-km-long Nam Ma fault runs approximately N70° E from the Yunnan to Myanmar, appearing as a narrow fault zone from both the LANDSAT imagery and the SRTM topography (Fig. 2). Our geomorphic mapping suggests that both the northeastern and the southwestern end of the Nam Ma fault terminate in transtensional basins, where the fault splays into several left-lateral and normal horsetail faults.

In its central part, the Nam Ma fault offsets the Mekong River channel 12 ± 2 km left-laterally (Lacassin et al., 1998). The Mekong River forms a hairpin river loop immediately south of the Nam Ma fault trace, suggesting that the Nam Ma fault was once a right-lateral fault and may have accommodated about 30 km right-lateral motion before it reactivated as a left-lateral fault between 20 Myr and 5 Myr ago (Lacassin et al., 1998). Based on the regional tectonic history and the offset of the Mekong River, Lacassin et al. (1998) suggests the average slip rate of the Nam Ma fault is about 2.4 to 0.6 mm/yr. This long-term slip rate is about half of the Mengxing fault slip rate (4.8 to

1.2 mm/yr) estimated by the same study, but much faster than the average slip rate of the Mae Chan fault (0.3 to 0.075 mm/yr) in the Thailand area (Fig. 2).

The March 24, 2011 Tarlay earthquake (M_w 6.8) is the first destructive earthquake that struck the Thailand-Myanmar border since the beginning of the 20th century (Engdahl and Villasenor, 2002). The Tarlay earthquake occurred about four years after the M_w 6.3 earthquake in Laos (Fig. 2). The M_w 6.8 event caused at least 74 deaths, 125 injuries and over 3,000 displaced at the Myanmar region (OCHA, 2012). A preliminary assessment in the earthquake-affected area suggests that 12% of buildings were destroyed by the earthquake, while the other 32% became uninhabitable (OCHA, 2011). The earthquake was felt from Kunming to Bangkok and Yangon, over 1000 km from the epicenter (USGS, Significant earthquake archive, 2011).

The size and shallow depth (< 15 km) of the mainshock indicated that the causative fault may have ruptured the surface, and the proximity of mainshock and aftershocks' epicenters to the left-lateral Nam Ma Fault suggested the rupture of a known fault (Fig. 2). Thus, a survey team from the Myanmar Earthquake Committee (MEC) and the Department of Meteorology and Hydrology of Myanmar (DMH) conducted a brief reconnaissance survey at the western part of the Nam Ma fault about two weeks after the earthquake. The main purpose of this reconnaissance survey was to confirm the source of the event, and to document the surface failure soon after the earthquake since most of the offset features may disappear or be altered after the earthquake.

In the pages that follow, we describe our field observations of the coseismic deformation along the westernmost part of the Nam Ma fault associated with the 2011 Tarlay earthquake. This is the first-of-its-kind field study in Myanmar. We also describe our finding from the post-quake high resolution satellite (HRS) imagery. We then discuss the preservation of coseismic deformation features via comparing the field observation and the interpretation of the satellite imagery, and the earthquake potential of the Nam Ma fault.

Field Observations

Logistics, scope of reconnaissance and methods

The part of the Shan Plateau we studied consists of small, cultivated valleys nestled among heavily forested, hilly terrain. The general inaccessibility of the hilly tracts, due to recent rain after the earthquake, led us to focus our 5-day (April 6 to April 10) reconnaissance along roads and in accessible valleys. Thus, our documentation focuses on flat, cultivated terrain within the hilly area (Fig. 3).

In addition to mapping and measuring the fault rupture, we also documented damage to manmade structures and non-tectonic ground failure, such as liquefaction and landslides (Fig. 3). Readers interested in these aspects of the earthquake may visit the electronic supplement to this article, which contains the surveyed waypoint locations and the associated field photographs.

Due to the lack of precise survey instruments (e.g., total stations) immediately after the earthquake, we used a tape measure and compass to measure the strike-slip offsets parallel to the observed average local strike of the fault rupture. We did not attempt to make formal estimates of measurement uncertainties during our short reconnaissance investigation. Rather, we selected offset reference lines (e.g., edges of paddy fields, channels) with the least irregularity and locations where the fault rupture appeared to be the simplest. In general, we believe the measurement errors are less than 10% of the measured value at the place where the fault rupture is clean. However, if tectonic warping near the fault rupture is significant, we are likely underestimating the amount of fault offset by several tens of centimeters. We used a hand-held GPS receiver to determine the location of each measurement and usually recorded the location after the GPS displayed a minimum error.

Field measurements

In this section, we describe the offsets from 47 sites that exhibited tectonic ground rupture. Additional information for these sites is available in the electronic supplement to this article. We begin with the site that exhibited the clearest evidence of tectonic offsets: the paddy fields west-southwest of Kya Ku Ni (Fig. 3).

Kya Ku Ni

The westernmost measurements are from paddy fields approximately 16 km southeast of the USGS epicenter. The trace of the rupture trends northeastward and is particularly clear along a 2-km section of the valley floor west of the Kya Ku Ni (Fig. 4). The rupture exhibits classical left-lateral slip features (Yeats et al., 1997): right-stepping en echelon Reidel shears, clear sinistral offsets of manmade features such as paddy berms and tire tracks, and several centimeters of vertical displacement (Fig. 5). The displacements are large enough to have produced a moletrack (Fig. 5).

Figure 4 shows a map view of the survey locations and 34 measurements along this stretch of paddy fields. Along the central part of the surveyed section, the left-lateral offsets vary by one order of magnitude, from 12 to 125 cm (Table 1). Over 90% of the measured displacements exceed 45 cm, and the average value is 81 cm. We did not find any systematic change in the sinistral offset along this 1-km-long section. We measured offsets of ~1.2 m at three different localities along the rupture; between these localities, sinistral offsets were smaller. Our field observations show some of these small offsets are associated with tectonic warping within several meters of the moletrack (e.g., Fig. 5d). Such off-fault warping may partly explain the large variation in offsets along this short section of the fault, as previous studies have suggested for other recent strike-slip ruptures (e.g., Rockwell et al., 2002; Rockwell and Klinger, 2011). Nevertheless, the multiple observations of large offsets indicate that the maximum sinistral offset for this section is approximately 1.25 m.

We found no clear measurable offset features in the paddy fields west of the westernmost recorded observations (Waypoint 364; Fig. 4). The moletrack was clear up to 400 m west-southwest of the westernmost measured offset at the Kya Ku Ni site (Fig. 4). Some of the paddy berms were clearly disrupted by the moletrack (Fig. 5e). Unfortunately, these field boundaries were highly oblique to the moletrack and were clearly warped across the wide rupture zone; we were unable to directly measure these offsets. We did not attempt to follow the rupture farther west into uncultivated hills. However, the analysis of the optical HRS imagery suggests the rupture extends at least 3 km westward beyond our last surveyed point (Fig. 3).

Pu Ho Mein

The cultivated valley near Pu Ho Mein village was easily accessible and we were able to observe how the fault rupture extended from the Kya Ku Ni area. Figure 6 shows locations of ground failure.

We found a small number of sites with tectonic fractures in this vicinity. Many localities clearly experienced ground failure, but none was convincingly tectonic. Most of these locations were on the southern slope of the valley, south of the fault trace mapped from the SRTM dataset and other optical satellite images (Fig. 6). Because of the dense vegetation on the hill slope, we were unable to make continuous observations following the surface rupture over this approximately 2-km-long section. Instead, we connect our surveyed tectonic fracture locations to map the extent of the fault rupture.

Compared to the Kya Ku Ni areas, the surface fault slip was much smaller at the Pu Oh Mein site. Approximately 2.4 km southwest of the village, we observed right-stepping en-echelon cracks trending 70° across a field (Waypoint 533; Fig. 7a, b). Although these en-echelon cracks disrupted the paddy berms in the field, no measurable offsets were found at these field boundaries (Fig. 7a). The lack of a clear moletrack and the small amounts of crack opening suggest that the sinistral offset at this location was no more than 10 or 20 cm near the surface. Approximately 1 km southwest of the town (Waypoint 522, 523), a series of right-stepping en echelon cracks suggest a few cm of sinistral slip across the fault (Fig. 7c, d). These observations suggest that the fault slips are relatively minor along the shallow part of the fault, where the surface deformation may be dominated by rotation and warping near the rupture.

Not all of the ground fissures that we mapped in Pu Ho Mein area can be linked by a single line of rupture. For example, we observed several ground fissures develop within about three hundred meters from the projection of the fault rupture at the Pu Ho Mein village. The orientation of these fissures is similar to the strike of the fault; thus we cannot exclude the hypothesis that these fissures are resulting from secondary faulting within the fault damage zone.

Tarlay

Northeast of Pu Ho Mein, we find the fault rupture near the Tarlay Township (Fig. 8). Comparing with the evidence at Kya Ku Ni area, the evidence for tectonic rupture was more subdued, and the magnitude of left-lateral slip was substantially less than at Kyi Ku Ni. Among these other sites, the ruptures near the Tarlay Township were the largest. Most of the observed ground failure was related to slumping and liquefaction along riverbanks. Away from the river, standing water in rice paddies and the height of the rice crop made tracing the rupture more difficult than in the drier paddy fields west of Kya Ku Ni. In Tarlay, the amount of slip was much smaller, so there were no moletracks or vertical displacements to help guide our search.

In general, most of the observed ground-failure locations are aligned with the fault rupture that we mapped from the western foothills (Fig. 3). However, the fault ruptures east of Tarlay do not match the pre-existing geomorphic features that we mapped from the LANDAT imagery. Instead, the fault rupture lies ~200 meters south of our pre-mapped fault trace, where the surface is covered by young and loose fluvial deposits along the Nam Lam River (Fig. 8).

Four locations within 2 km along the projected fault trace, based upon our mapping of the fault using SRTM topography and LANDSAT imagery, exhibit left-lateral displacements of 15 to 53 cm. The westernmost site (Waypoint 293) yielded the largest offset, but its offset is complex and was in the earthen abutment of the Tarlay Bridge. The stone bridge across the Nam Lam River experienced minor damage (Fig. 9a). At the southern end of the bridge, the eastern side of the abutment displayed a simple, 53-cm sinistral offset. The sinistral offset on the western side of the abutment was much smaller, but the slip sense is consistent with the left-lateral slip observed at the eastern side of the bridge. This offset cannot be explained by failure of the embankment fill and likely reflects tectonic offset.

Approximately 600 m northeast of the bridge, there were clear 40-cm sinistral offsets of a narrow irrigation channel and its two shoulders (Waypoint 547; Fig. 9b). Our observation also suggests that near the rupture trace was significant surface warping that we can’t measure in the field. Approximately 1.2 km farther northeast were two fractures that offset a paddy embankment by a total of 37 cm (Waypoint 577; Fig. 9c), showing the distributed deformation along the fault trace. Two fractures 500 m to the northeast strike substantially more northerly (30° to 70°) than the overall strike of the fault zone, with sinistral offsets of 36 and 15 cm. Another 300 m to the northeast, the offset in the paddy edge suggests 15 cm of sinistral offset along the projected surface rupture (Waypoint 609; Fig. 9d). We also found two enigmatic, but sharp, normal-dextral offsets in a paddy berm just south of the offset at Waypoint 609. These two offsets were oriented differently (30°) than the general strike of the fault (70°) and correspond to a right-lateral offset of the field boundary of 10 and 13 cm, respectively. We suspect these normal-dextral offsets are part of the en-echelon fractures south of the main fault rupture. However, we cannot trace their extent in the rice paddies.

The field survey team also visited two sites (Waypoints 276, 290) at the northern edge of the Tarlay basin, where the main trace of the Nam Ma Fault was apparent in the geomorphology (Fig.

3; Fig. 8). Observations at both sites suggest that this part of the main surface trace of the Nam Ma Fault experienced only very minor, if any, fault slip during the 2011 earthquake.

One of these sites is east of the town of Tarlay, where several discontinuous fissures developed along a road that is nearly parallel to the Nam Ma Fault (Waypoint 276; Fig. 8). One of these fissures cut across a bamboo fence in a field; however, no offset or bend in the fence was observed across the fissure (Fig. 10a). The second site is at the mountain front northwest of Tarlay (Waypoint 290; Fig. 8), where two nearly parallel ground fractures developed during the earthquake according to the villager. These fractures trend about N30E. The northern fracture showed no sign of offset where it crossed the boundary of a paved road (Fig. 10b). The other fissure, on the bottom of a fishpond south of the road, displayed no disruptions along the pond's bank.

The lack of offset features along the main trace of the Nam Ma Fault suggests that the fault at the northern edge of the basin did not play an important role in the March 2011 earthquake. Most of the observable ground failures were within the flat basin area, where they developed along the eastern projection of the fault trace southwest of the town of Tarlay.

Eastern end of the rupture

Two areas to the northeast of Tarlay display sinistral offsets that are approximately along the projection of the fault trace from the southwest. Because we found only two disturbed locations that are far apart, we are not sure whether the easternmost survey locations reflect tectonic rupture. Figure 11 shows these two locations along the northeastern extension of the surface rupture observed at Tarlay. At Waypoint 327, we measured a 20-cm sinistral horizontal offset and a 20-cm vertical offset down to the south at the edge of a paddy (Fig. 12a). Nearby, at Waypoint 325, the measured sinistral offset is 30 cm and the vertical offset is several centimeters (Fig. 12b).

The ruptures at these two locations strike roughly parallel to the general strike of the surface rupture and are aligned with other surface ruptures extending from the Tarlay area. These fractures may represent the northeastern-most extent of tectonic rupture in 2011.

Farther northeast, we observed a group of ground failures associated with considerable liquefaction (Waypoint 302 to 311; Fig. 11). Most of the fractures had a clear dip-slip component, but none exhibited clear sinistral offset. We measured vertical offsets of 15 cm at Waypoint 302 (Fig. 12c) and 40 cm at Waypoint 311, with a clear northward tilting near the fracture (Fig. 12e). These may be tectonic in origin, but they are so small that we cannot be certain. Also, the strikes of these features (approximately 20°) differed from the general orientation of the rupture (70°), which makes their origin uncertain. In fact, the widely distributed liquefaction suggests intense reworking of near-surface sediments along these surveyed cracks, thus we can not exclude the possibility that these surface cracks are resulting from the sand ejection and ground compaction during the earthquake.

Remote sensing observations

Kya Ku Ni and further west

To complement our field survey, we also use the post-quake high resolution satellite (HRS) images to study and quantify the fault rupture along the westernmost segment of the Nam Ma fault. The spatial resolution of the HRS images (WorldView-2) is about 0.5 m, and they were collected between Feb 2012 and Feb 2013. We especially focus on the area near the Kya Ku Ni and further southwest, as our survey shows the left-lateral offset at this location is large enough (> 0.5 m) to be measured from the images. We also search the area near Pu Ho Mein and the area northeast of Tarlay, to see if there are any preserved fault traces that we did not map during our reconnaissance survey in April 2011.

At the Kya Ku Ni site, our mapping shows that about 8 paddy field boundaries still preserve a measurable left-lateral deflection in the Sep 2012 image. The left-lateral displacements measured from the Sep 2012 image range from 1.1 to 1.6 m at Kya Ku Ni section (Fig. 3). These remote measurements are systematically higher than the field survey results from Apr 2011, but within the uncertainty of our HRS imagery (±0.5 m; e.g., Klinger et al., 2005).

West of the Kya Ku Ni area, our mapping from HRS image suggests that the fault rupture extends at least 3 km further southwest from our last surveyed point (Fig. 3). The comparison of the pre-quake HRS image from the Google Earth and the 2013 WorldView-2 image shows that the rupture clearly transects through the paddy fields west of the Kya Ku Ni surveyed sites, showing a nearly one-km-long moletrack in the field (Fig. 13a). The paddy field boundaries and roads across the rupture show clearly left-lateral deflections in both the 2012 and 2013 HRS images. Our measurements from the HRS images suggest that most of the left-lateral offsets are about 1 to 1.5 m, whereas the maximum left-lateral offset is 2.5 ± 0.5 m at one location. The average 1 to 1.5 m left-lateral offset is similar to the estimation from the pixel-tracking analysis of the L-Band radar image (Wang et al., 2013), and similar to the measurements at Kya Ku Ni site. We also notice that two small sag ponds appear at the north side of the moletrack, suggesting the block north of the fault was dropped down approximately 10-20 cm during or after the earthquake. Further west, the rupture trace becomes unclear in the HRS images. Only few paddy field boundaries still show left-lateral deflection two years after the earthquake.

Figure 13b shows the western-most location where we are able to confirm the fault rupture from the 2013 HRS image, about 3 km from the last surveyed point at the Kya Ku Ni site. The rupture transects through a narrow river valley and forms a sag pond northwest of the fault trace. We estimate the left-lateral offset to be about 1 m from the left-lateral deflection of one paddy field berm. The fault rupture soon propagates into the mountains west of this point and can hardly be traced from the satellite image. Approximately 3 km further west, about 6 km southwest of our last field observation point, another E-W running scarp appears in the 2013 HRS image that we suspect to be the 2011 fault rupture. However, we are not able to identify any offset feature along the scarp as the field boundaries are nearly parallel to the suspect scarp (Fig. 13c).

Discussion

Compilation of results

The left-lateral and vertical-slip distributions of the 24 March 2011 earthquake rupture are presented in Figure 3, which shows the 46 left-lateral offsets that were recorded in the field, and 26 left-lateral offsets that were mapped from 2012 and 2013 HRS images. We interpret all but the easternmost two field measurement (Waypoints 302 and 311) to be tectonic in origin. Table 1 lists data relevant to these field measurements.

Difficult logistics prevented a comprehensive post-earthquake survey of the entire rupture during the 5 days in the field. Nevertheless, the data we collected suggest that the amount of left-lateral offset decreased gradually northeastward from more than a meter near Kya Ku Ni to several tens of centimeters east of Tarlay.

Among our field observations, we find most of the surface ruptures within the Tarlay basin accompanied by significant surface warping near the fault, especially in the water-saturated rice paddy fields. Field observations suggest that the surface warping sometimes occurred over ten meters from the fault rupture (e.g., Fig. 9b), which makes it difficult to measure the tectonic warping without knowing its original geometry before the earthquake. Thus our measurements within the Tarlay basin likely underestimate the tectonic offset across the fault trace. Alternatively, we suggest the horizontal offsets near the fault are smaller than one meter in the Tarlay basin, as we can not observe any paddy field berms' left-lateral deflection from the HRS imagery. If the tectonic displacements in the Tarlay basin are greater than one meter, such as in the fault offsets west of the

Kya Ku Ni village, we should be able to observe left-lateral deflections on the features that cross the fault unless the displacement is highly distributed.

Our observations also showed that the block south of the fault dropped along most of the surveyed sections, with few exceptions west of Kya Ku Ni. This observation agrees with the moment tensor solution for the Tarlay earthquake from the Global CMT project, which indicates that the fault-slip plane dips steeply to the south and has a very minor normal-slip component.

The rupture length of the 2011 Tarlay earthquake

Our field survey results and remote sensing interpretation imply that the total rupture length is at least 19 km during the 2011 earthquake (Fig. 3). The ruptures primarily follow a previously mapped fault segment along the westernmost part of the Nam Ma Fault (Fig. 2; Fig. 3). The western end of this fault segment is approximately 9 km west of our westernmost survey point, and its eastern end is within a basin that reflects a 5-km-wide dilatational stepover of the Nam Ma Fault. The 2011 rupture was confined within this westernmost section of the Nam Ma Fault, which encourages us to consider the length of the fault segment as the maximum rupture length of the Tarlay earthquake.

Based on the geomorphological evidence from the 90-m SRTM, 15-m Landsat imagery and 0.5-m HRS images, the fault trace does not extend more than 9 km southwest from our southwesternmost measurement. We did not observe any other faults in the remote sensing dataset near the southwestern tip of the ground rupture. Therefore, the southwestward extension of the surface rupture could not exceed the tip of the fault. To the northeast, the surface rupture most likely terminates between Waypoints 327 and 304 in the center of the basin. If the fault terminated very close to Waypoint 304, the rupture would not extend more than 5 km northeast of our easternmost measurement point (Waypoint 327). As a result, the maximum plausible surface rupture length of the Tarlay earthquake is 30 km from the western hills to the basin.

Our estimate of the fault rupture length is very similar to that based on the earthquake magnitude and the empirical relationship from Wells and Coppersmith (1994). On average, a shallow M_w 6.8 strike-slip earthquake produces an approximately 30-km-long surface rupture and about 1 m of maximum surface displacement (Wells and Coppersmith, 1994). The similarity between our interpretation and the global data suggests that the entire westernmost segment of the Nam Ma fault ruptured during the 2011 M_w 6.8 Tarlay earthquake.

Preservation of offset features

Our analysis of post-earthquake HRS images suggests that most of the offset features, if not all, become invisible in the paddy fields east of the Kya Ku Ni area about 1 year after the earthquake. At the Kya Ku Ni site, we found that about half of the offset features that experienced more than 80 cm offset disappeared within 1.5 years after the earthquake. This observation suggests most of the offset features that experienced less than 1 m horizontal displacement in a similar agricultural environment may soon disappear after the earthquake. For features that show about 1 to 1.5 m horizontal displacement, our observation from the HRS images suggests they are commonly modified by the famers, but still retain the general left-lateral deflection across the fault even 2 years after the earthquake. Thus, we are still able to measure their horizontal displacement 1.5 to 2 years later, with a similar outcome to the field survey results obtained right after the earthquake (Fig. 3).

At some locations, we find that not only the offset paddy field boundaries and roads were preserved, but also the fault rupture trace remained visible in the cultivated fields from the satellite imagery. One example is the site just west of Kya Ku Ni, where the left-lateral displacements are similar to those at the Kya Ku Ni area (Fig. 3). Although both of these sites share similar left-lateral displacements, the fault rupture traces at Kya Ku Ni had completely disappeared in the Sep 2012 image, while the adjacent section is still visible in the paddy fields (Fig. 13a).

We attribute this different degree of preservation to vertical displacement of the fault. At the Kya Ku Ni site, our field observations suggest that the vertical displacement was very minor across the fault; therefore we believe that the farmers could easily fix the fault rupture before the coming growing season. To the west, our mapping from 2012 and 2013 HRS images suggests that the block north of the fault dropped several tens centimeters along the preserved fault trace. It is likely that the farmers tend to convert these rupture traces to the field boundaries and thus the fault traces were preserved in the field.

Seismic potential of the rest of the Nam Ma Fault

Only the westernmost 20 to 30 km of the Nam Ma Fault ruptured during the 2011 Tarlay earthquake. The rest of the 215-km-long Nam Ma Fault has not been associated with any major earthquakes for at least the past century. The historical earthquake record in Thailand suggests that the last major event that struck the nearby Chiang Rai city was in A.D. 1715 (Bott et al., 1997). This more-than-a-century-long quiescence of the fault suggests significant stress accumulation in the blocks bounding the majority of the Nam Ma Fault.

For the westernmost 30-km-long segment of the Nam Ma fault, we can estimate the frequency of Tarlay-like earthquakes by calculating the seismic moment accumulation rate on the given fault plane. We consider that the fault plane that generates the Tarlay earthquake is 30 km long, and the downdip limit of the rupture patch is similar to the locking depth of the central Sagaing fault, at 15 km in depth (Vigny et al, 2003). We also adapt the 2.4 to 0.6 mm/yr averaged Nam Ma fault slip rate from Lacassin et al. (1998) and a reference crustal shear modulus of 32 GPa to calculate the seismic moment accumulation rate on the given fault plane. Our result suggests that the westernmost segment of the Nam Ma fault can produce an M_w 6.8 earthquake about every 600 to 2300 years, depending on the slip accumulation rate on the fault plane. This 600 to 2300 year interval is very close to the estimated interval (520 to 2100 years) from the field observed maximum surface offset (1.25 m), but as twice long as the recurrence interval (260 to 1050 years) estimated from the predicted average displacement (0.63 m) of an M_w 6.8 earthquake from Wells and Coppersmith (1994).

The rest of the Nam Ma fault may capable of generating a M_w 7.7 to 7.8 earthquake if the rest of ~195 km long fault ruptured at once (Wells and Coppersmith, 1994; Blaser et al., 2010). By assuming the same fault rupture width (15 km) and the slip rate (2.4 to 0.6 mm/yr) throughout the entire Nam Ma fault, we expect that a magnitude 7.7 earthquake would occur approximately every 1800 to 7200 years on the 215-km-long Nam Ma fault. Whether this type of earthquake occurred on the Nam Ma fault or not is currently unclear, as the information of historical earthquakes is spotty and only covers a short period of time (Bott et al., 1997). Future paleoseismological study will significantly improve our knowledge of the Nam Ma fault slip behavior.

Conclusions

Our field observations confirm that the westernmost segment of the Nam Ma Fault caused the Tarlay earthquake of 24 March 2011. This is the first time that any coseismic fault surface ruptures have been mapped in the Myanmar area after an earthquake. The N70E trending surface ruptures are consistent with the Global CMT parameters for the earthquake. Field observations confirm that fault slip was almost purely sinistral, with minor dip-slip displacement along the fault rupture. The observed maximum offset of 1.25 m occurred approximately 9 km west of the western end of the topographically defined fault trace. The amount of sinistral offset decreased gradually eastward before terminating within the Tarlay Basin, along the southern edge of a 2-km-wide releasing stepover of the Nam Ma fault.

Our observations suggest that the surface rupture extends more than 19 km along a 30-km-long, previously mapped fault segment that is structurally distinct from the main trace of the

Nam Ma Fault. If this entire fault segment slipped during the mainshock, the maximum rupture length is likely to be about 30 km from the foothills west of the town of Tarlay to the dilatational basin. This is very similar to the average length of surface ruptures for an M_w 6.8 earthquake. Judging from the lack of observed rupture along other sections of the fault and the similarity of the rupture length to the global dataset, we believe the westernmost segment of the Nam Ma fault is solely responsible for the Tarlay earthquake. Such an earthquake may recur on the same section of the fault every 600 to 2300 years, based on the long-term slip rate of the Nam Ma Fault. The rest of the Nam Ma fault is capable of generating an M_w 7.7 to 7.8 earthquake if the fault ruptured all at once. Future paleoseismological study is important to improve our understanding of seismic hazard in this area.

Data and Resources

Earthquake epicenters used in this study were collected from the NEIC PDE catalog: http://earthquake.usgs.gov/earthquakes/eqarchives/epic/ (last accessed Nov 2011). The CMT solutions were obtained from the Global Centroid Moment Tensor Project database using www.globalcmt.org/CMTsearch.html (last accessed Nov 2011).

The digital elevation data were obtained from the SRTM 90m database: http://srtm.csi.cgiar.org/ (last accessed: June 2012). The Landsat imagery is collected from the USGS Earth Resources Observation and Science Center (EROS) searched using http://glovis.usgs.gov/ (last access June 2012).

Acknowledgments

We deeply appreciate the assistance of the Venerable U Wazibate, who supplied our field party with a four-wheel-drive vehicle. We greatly appreciate the Public Works Department

(Ministry of Construction), the Department of Meteorology and Hydrology (Ministry of Transport) and Ahkhar ethnic leaders in Tachileik City for their assistance in field planning. We also thank Paul Tapponnier and Yves Descatoire for their help in guiding our fieldwork in the days after the earthquake. Discussion with Win Swe helped improve the quality of the manuscript. Financial support for the field reconnaissance came from the Myanmar Geosciences Society, the Myanmar Engineering Society, the Myanmar Earthquake Committee, Resource & Environment Myanmar Co. Ltd. and Thingazar Tours.

References

Blaser, L., F. Kruger, M. Ohrnberger & F. Scherbaum (2010), Scaling relations of earthquake source parameter estimates with special focus on subduction environment, Bull. seism. Soc. Am., 100(6), 2914–2926.

Bott, J., I. Wong, S. Prachuab, B. Wechbunthung, C. Hinthong and S. Surapirome (1997), Contemporary seismicity in northern Thailand and its tectonic implications, In: Dheeradilok, P., (Ed.), Proceedings of the International Conference on Stratigraphy and Tectonic Evolution of Southeast Asia and the South Pacific, Department of Mineral Resources, Bangkok, 453 – 464.

Curray, J., D. Moore, L. Lawver, F. Emmel, R. Raitt, M. Henry, and R. Kieckhefer (1979). Tectonics of the Andaman Sea and Burma, Am. Assoc. Pet. Geol. Mem., 29 189-198.

DeMets, C., R.G. Gordon, and D.F. Argus (2010), Geologically current plate motions, Geophys. J. Int., 181(1), 1-80, doi: 10.1111/j.1365-246X.2009.04491.x.

Engdahl, E.R. & A. Villasenor (2002), Global Seismicity: 1900–1999, International Handbook of Earthquake and Engineering Seismology, v. 81A, Elsevier Science Ltd., Amsterdam, The Netherlands, 665–690.

Holt, W. E., J. F. Ni, T. C. Wallace, and A. J. Haines (1991), The active tectonics of the eastern Himalayan syntaxis and surrounding regions, J. Geophys. Res., 96(B9), 14595–14632, doi:10.1029/91JB01021.

Klinger, Y., X. Xu, P. Tapponnier, J. V. der Woerd, C. Lasserre and Geoffrey King (2005), High-Resolution Satellite Imagery Mapping of the Surface Rupture and Slip Distribution of the Mw ~7.8, 14 November 2001 Kokoxili Earthquake, Kunlun Fault, Northern Tibet, China, Bull. Seism. Soc. Am. 95(5) 1970-1987.

Kreemer, C., W.E. Holt, and A.J. Haines (2003), An integrated global model of present-day plate motions and plate boundary deformation. Geophys. J. Int., 154: 8–34. doi: 10.1046/j.1365-246X.2003.01917.x.

Lacassin, R., A. Replumaz, and P. Herve Leloup (1998). Hairpin river loops and slip-sense inversion on southeast Asian strike-slip faults, Geology, 26(8) 703-706.

Le Dain, A., P. Tapponnier, and P. Molnar (1984). Active faulting and tectonics of Burma and surrounding regions, J. Geophys. Res., 89(B1) 453-472.

Nielsen, C., N. Chamot-rooke and C. Rangin (2004). From partial to full strain partitioning along the Indo-Burmese hyper-oblique subduction: Mar. Geol. 209 303-327.

OCHA (2011) Myanmar: Earthquake in Shan State Situation Report No. 6, UN Office for the Coordination of Humanitarian Affairs.

OCHA (2012) Myanmar: Natural Disasters 2002-2012, Map, UN Office for the Coordination of Humanitarian Affairs.

Prawirodirdjo, L. and Y. Bock, (2004), Instantaneous global plate motion model from 12 years of continuous GPS observations, J. Geophys. Res., 109, B08405, doi:10.1029/2003JB002944.

Rockwell, T. K., S. Lindvall, T. Dawson, R. Langridge, W. Lettis, and Y. Klinger (2002). lateral offsets on surveyed cultural features resulting from the 1999 Izmit and Duzce Earthquakes, Turkey, Bull. Seism. Soc. Am. 92(1) 79-94.

Rockwell, T.K. and Y. Klinger (2011). The variability of along-strike co-seismic slip: A new example from the Imperial fault of southern California. 2nd INQUA-IGCP-567 International Workshop on Active Tectonics, Earthquake Geology, Archaeology and Engineering, Corinth, Greece (2011), 200-203.

Sella, G. F., T. H. Dixon, and A. Mao (2002), REVEL: A model for recent plate velocities from space geodesy, J. Geophys. Res., 107(B4), 2081, doi:10.1029/2000JB000033.

Socquet, A., and M. Pubellier (2005), Cenozoic deformation in western Yunnan (China-Myanmar border), J. Asian Earth Sci., 24, 495–515.

Socquet, A., C. Vigny, N. Chamot-Rooke, W. Simons, C. Rangin, and B. Ambrosius (2006). India and Sunda plates motion and deformation along their boundary in Myanmar determined by GPS, J. Geophys. Res., 111 B05406.

Vigny, C., A. Socquet, C. Rangin, N. Chamot-Rooke, M. Pubellier, M.-N. Bouin, G. Bertrand, and M. Becker, (2003). Present-day crustal deformation around Sagaing fault, Myanmar, J. Geophys. Res., 108(B11), 2533, doi:10.1029/2002JB001999.

Wang, E., B. C. Burchfiel, L. H. Royden, L. Chen, J. Chen, W. Li, (1998), Late Cenozoic Xianshuihe-Xiaojiang and Red River fault systems of southwestern Sichuan and central Yunnan, China, Spec. Pap. Geol. Soc. Am., 327, 108.

Wang, Y.Z., E.N. Wang, Z.K. Shen, M. Wang, W.J. Gan, X.J. Qiao, G.J. Meng, T.M. Li, W. Tao, Y.L. Yang, J. Cheng and P. Li, (2008) GPS-constrained inversion of present-day slip rates along major faults of the Sichuan-Yunnan region, China. Science in China Series D: Earth Sciences, 51(9), 1267-1283.

Wang, Y., Y.-N. Lin, M. Simons, Soe Thura Tun, (2013), Shallow rupture of the 2011 Tarlay earthquake (Mw 6.8), Eastern Myanmar, Bull. Seism. Soc. Am. In review.

Win Swe (1970). Rift-features at the Sagaing-Tagaung ridge: In Proc. 5th Burma Research Congress, Rangoon.

Wells, D. L., and K. J. Coppersmith (1994). New Empirical Relationships Among Magnitude, Rupture Length, Rupture Width, Rupture Area, and Surface Displacement, Bull. Seism. Soc. Am. 84(4) 974-1002.

Yeats, R. S., K. Sieh, and C. R. Allen, (1997). The geology of earthquakes, New York, Oxford Univ. Press.

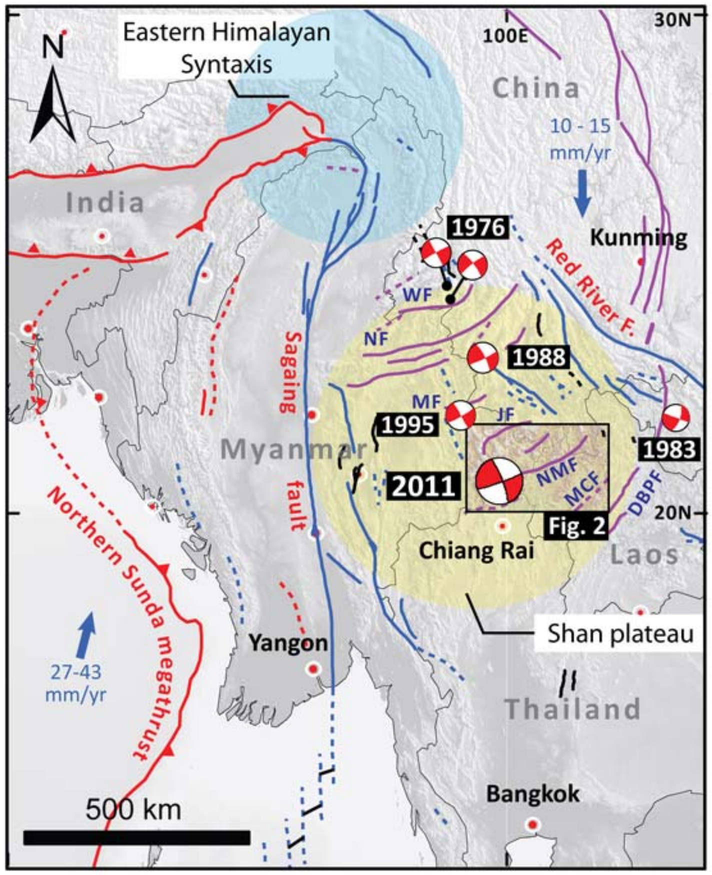

Figure 1. The neotectonic context of Myanmar and adjacent regions. The Shan fault system in eastern Myanmar lies between the Sagaing fault and the Red River fault, and is one of the three major fault systems that dominate the active tectonics of the Myanmar region. Its predominantly southwest-striking left-lateral faults span a 700-km wide section of the Chinese border with Vietnam, Laos, Thailand and Myanmar. The western part of the Nam Ma fault in the southern part of the Shan fault system produced the 2011 Tarlay earthquake. The active faults are based upon analysis of bathymetry and SRTM topography. Red line = reserves fault, Blue line = right-lateral fault, and purple line = left-lateral fault. The focal mechanisms of recent large (M_w >6.5, since 1976) earthquakes are from the Global CMT project. The plate motion rate relative to the Sunda plate is calculated from various plate-rotation models (Sella et al., 2002; Prawirodirdjo and Bock, 2004; Kreemer et al., 2003; Socquet et al., 2006; Wang et al., 2008; DeMets et al., 2010). WF: Wanding fault; NF: Nanting fault; MF: Menglian fault; JF: Jing Hong fault; NMF: Nam Ma fault; DBPF: Dien Bien Phu fault; CMF: Mae Chan Fault.

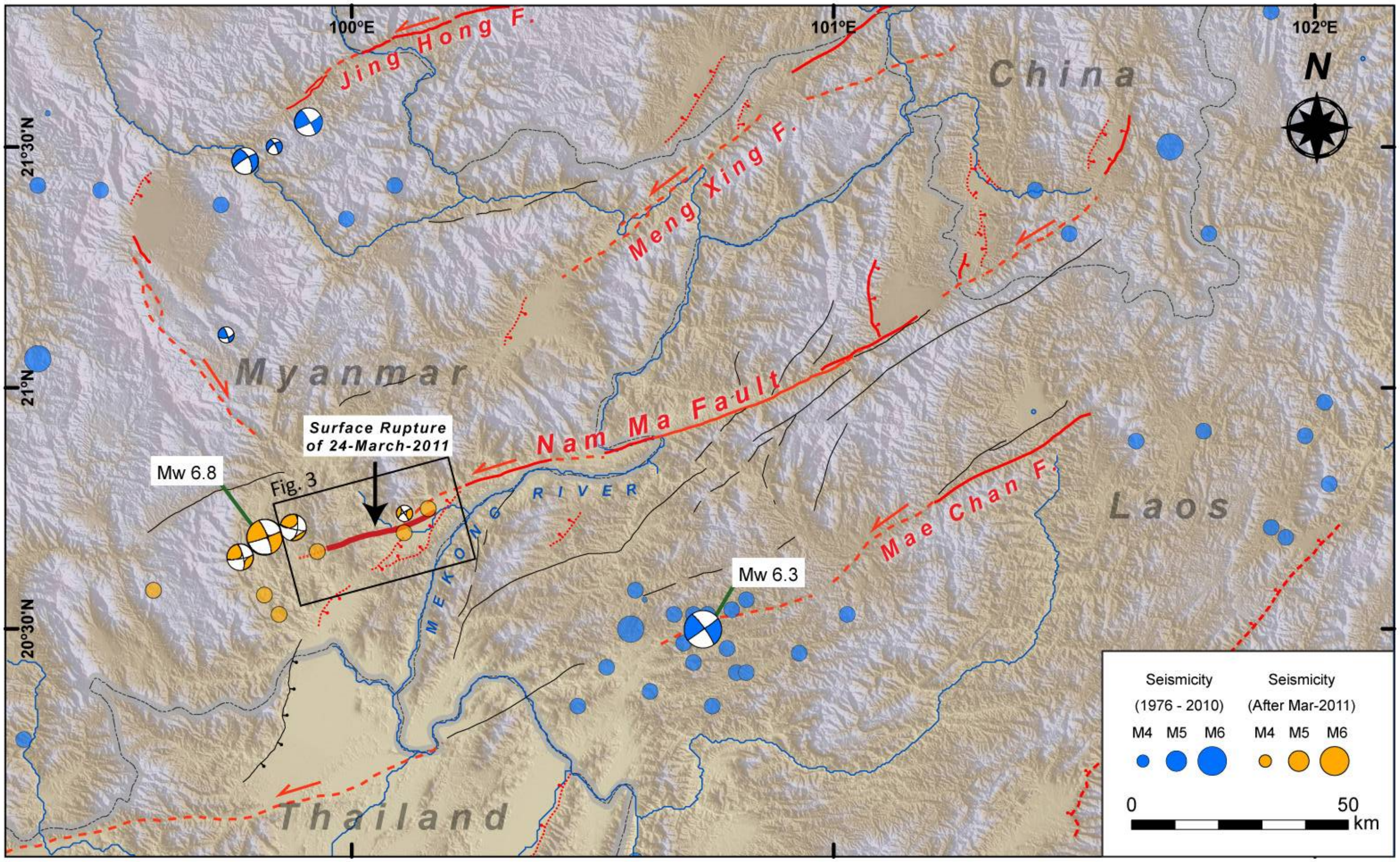

Figure 2. Map of the active faults around the Nam Ma Fault, based on geomorphological analysis of optical imagery and SRTM topography. The surface rupture in 2011 occurred along the thick bold line. The basemap is shaded 90-m SRTM topography.

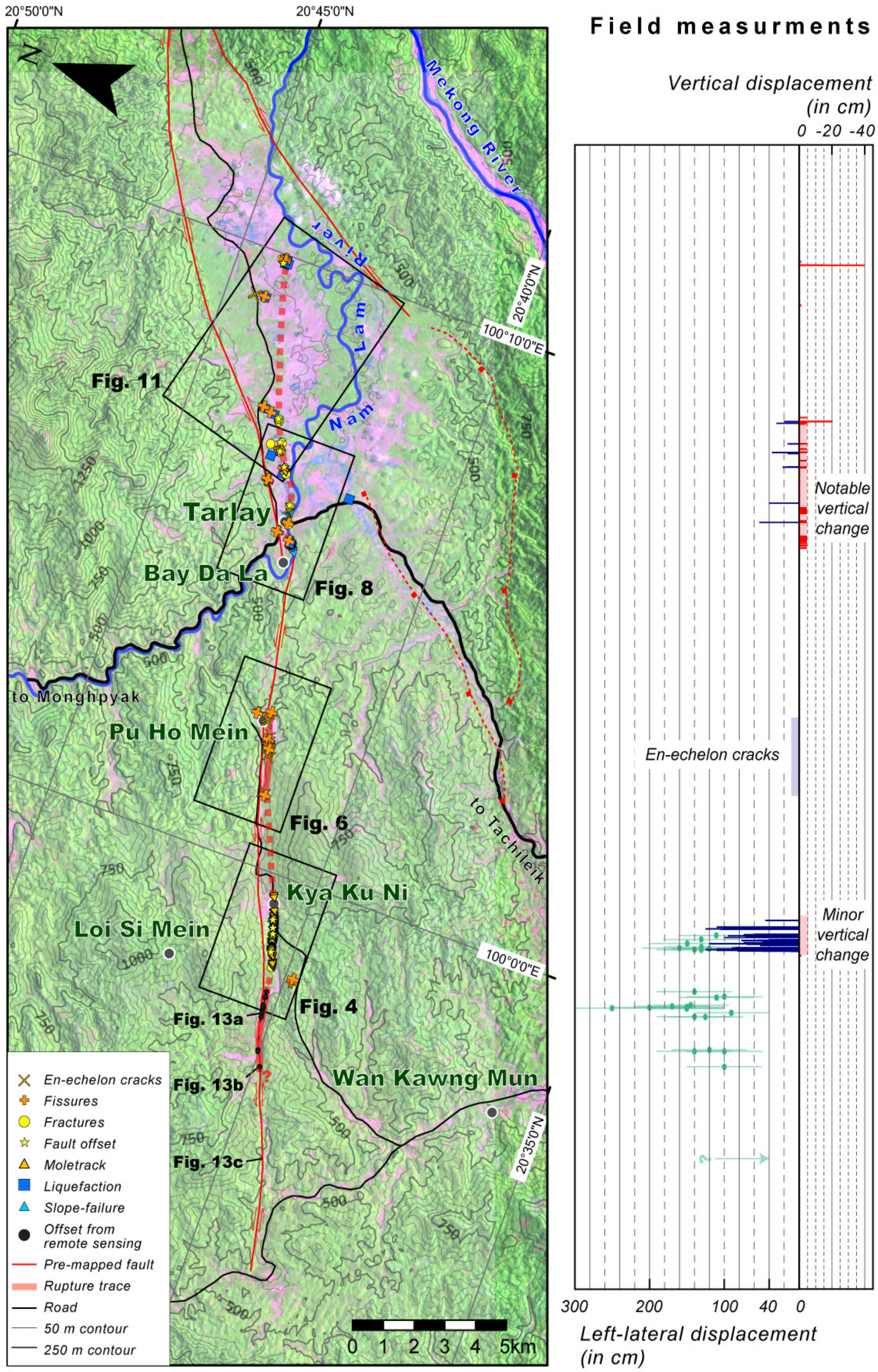

Figure 3. The surface rupture and surveyed locations for the 24 March 2011 Tarlay earthquake along the westernmost section of the Nam Ma Fault. The green dot shows the surface displacement measured from 0.5-m WorldView-2 images after earthquake. Blue

column is the field measurement result. Blue shaded area shows the area where we observe only en-echelon cracks along the fault. Red line is the vertical displacement measured in the field.

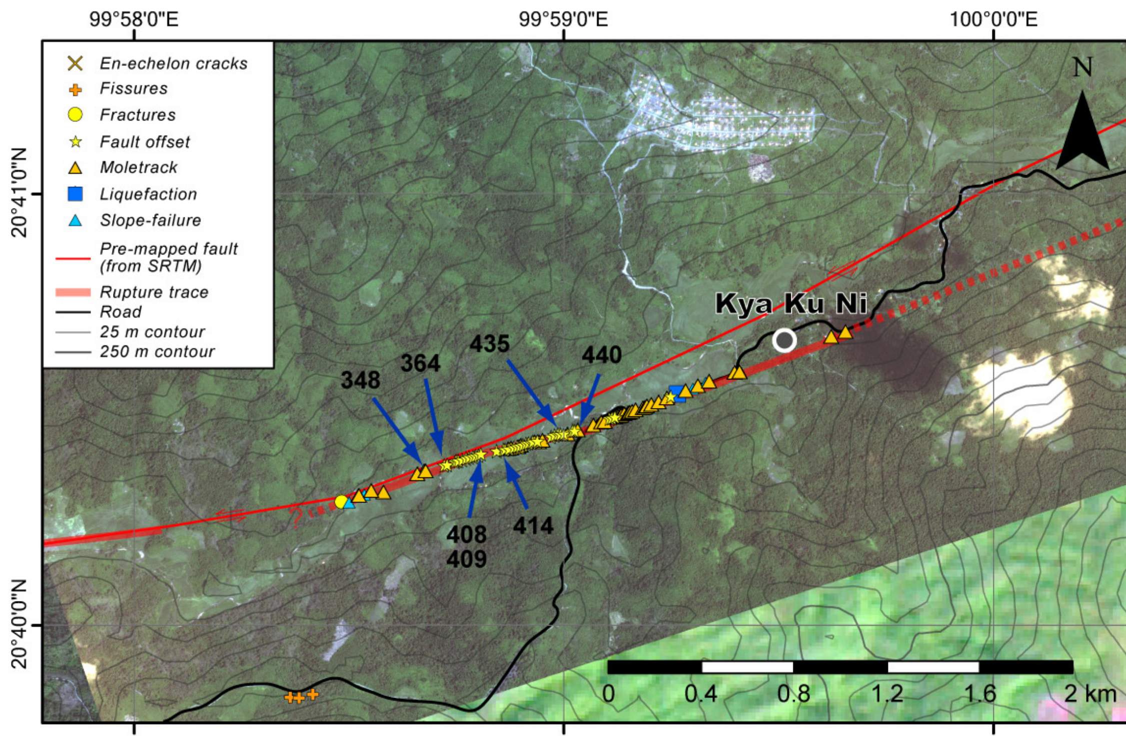

Figure 4. Map of the westernmost mapped fault rupture crossing paddy fields west of Kya Ku Ni village. The basemap is 0.5-m WorldView-2 imagery collected on Sep 29, 2012. The 25 m contour is generated from the 90-m SRTM dataset.

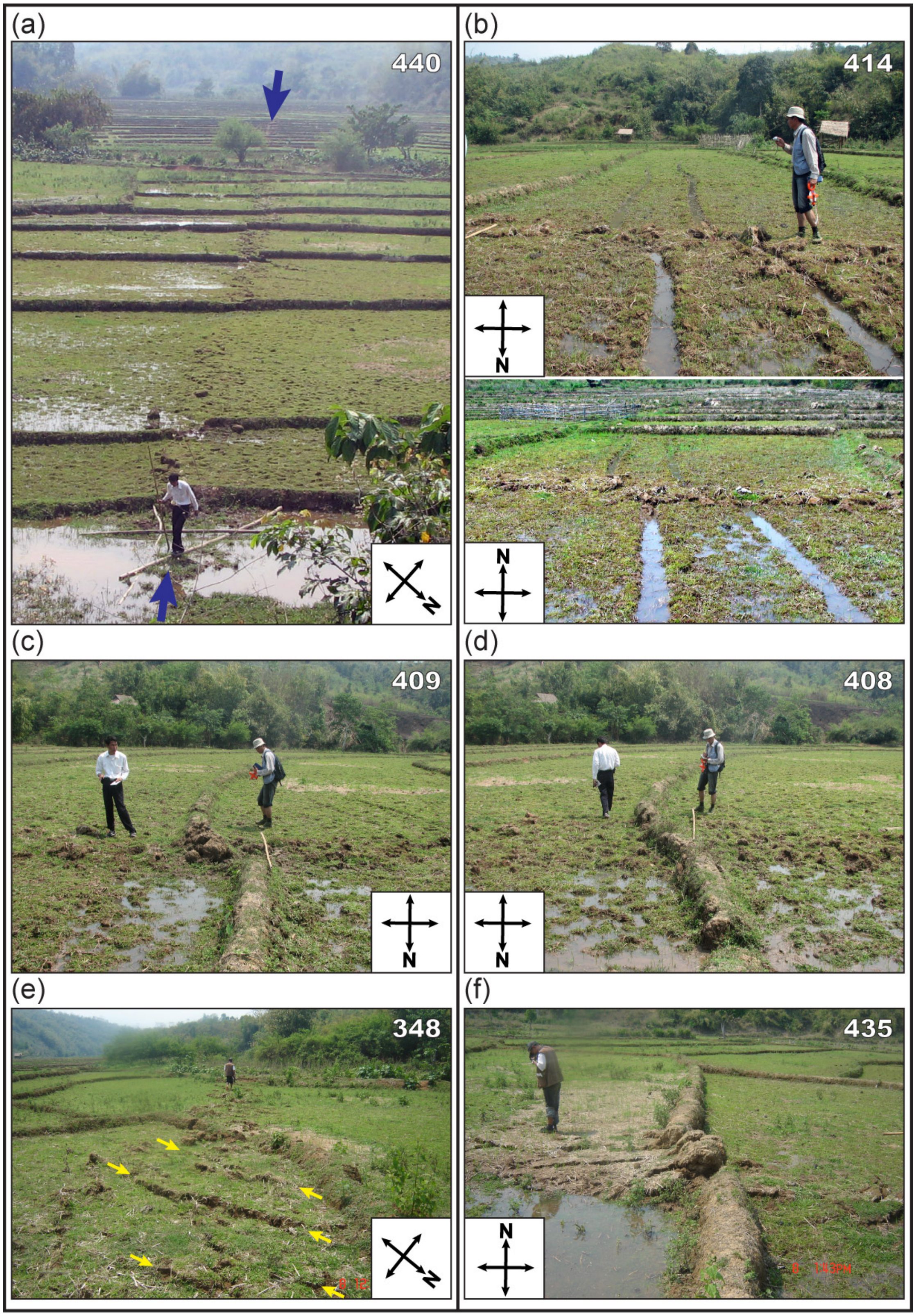

Figure 5. Photographs of the fault rupture in the paddy fields southwest of Kya Ku Ni.

(a) Overview of the rupture, looking southwestward from near Waypoint 440. Note the right-stepping Riedel shears, the moletrack and the small vertical component of slip implied by the water on the south (left) side of the fault rupture.
(b) 52-cm sinistral offset of two vehicle tracks at Waypoint 414, viewed from the south and the north. Note the likely tectonic warping of tracks on the far side of the fault in the upper photo.
(c) 85-cm sinistral offset and surface warping of the paddy boundary at Waypoint 409.
(d) 90-cm sinistral surface warping across the fault zone at Waypoint 408, just west of Waypoint 409. The paddy boundary is clearly warped across the rupture zone.
(e) 3-m-wide right-stepping Riedel shears zone at Waypoint 348.
(f) 72-cm left-lateral offset of a paddy divider near Waypoint 435. Note the subsidence of the south side, the moletrack and the right-stepping Riedel shears.

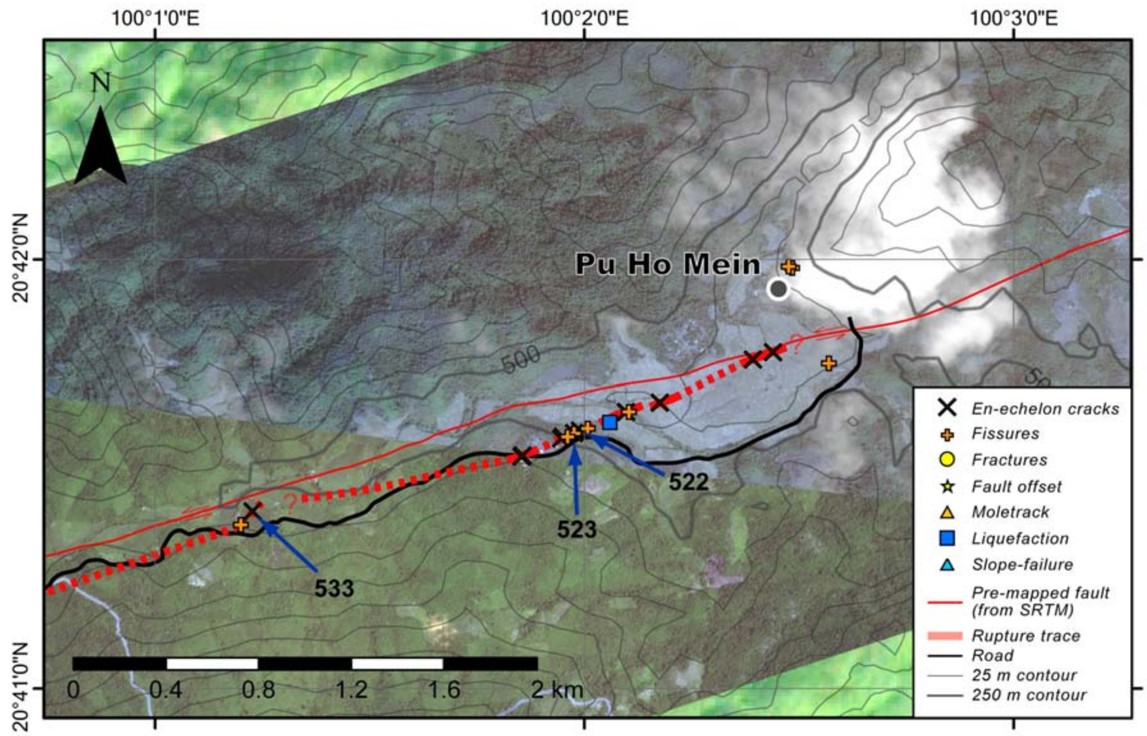

Figure 6. Map view of the area surrounding Pu Ho Mein village, showing locations of where we documented ground failure. Right-stepping en echelon cracks and other fractures suggest sinistral tectonic rupture. The basemap is from 0.5-m WorldView-2 imagery collected on Feb 12, 2012 and Sep 29, 2012. The 25 m contour is generated from the 90-m SRTM dataset.

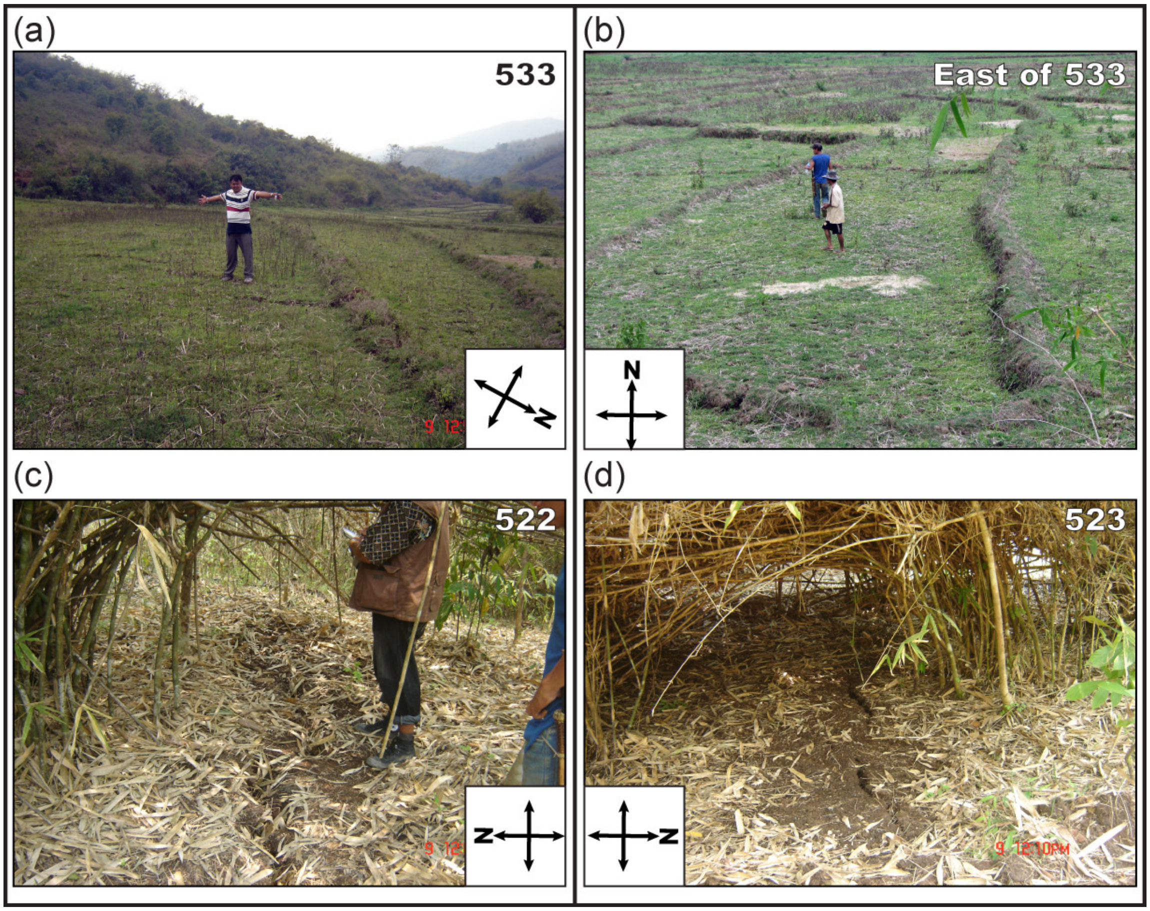

Figure 7. Photographs from three locations in the valley near Pu Ho Mein that may have experienced sinistral tectonic rupture.
(a) Right-stepping en echelon fractures across a dry paddy field at Waypoint 533.
(b) A long fracture and sand blows in paddy fields east of Waypoint 533.
(c) Right-stepping en echelon fractures at Waypoint 522 suggest a few cm of sinistral slip.
(d) Right-stepping en echelon cracks at Waypoint 523 suggest a few cm of sinistral slip.

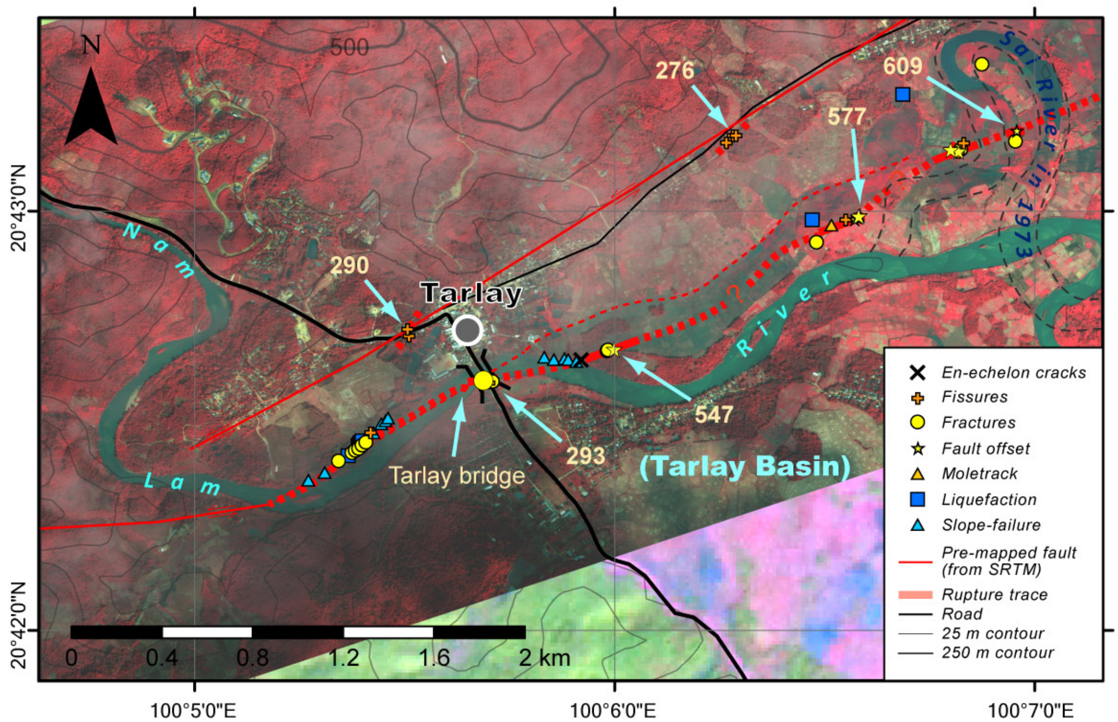

Figure 8. Map of sites inspected in the vicinity of the Tarlay Township, showing several locations of left-lateral offset, which coincide with other ground-failure locations along the Nam Lam River. The thin dashed line shows the inferred fault location south of Tarlay from the 15-m LANDSAT and other high-resolution satellite imagery. The basemap is the 0.5-m false-color WorldView-2 image collected on Feb 12, 2012.

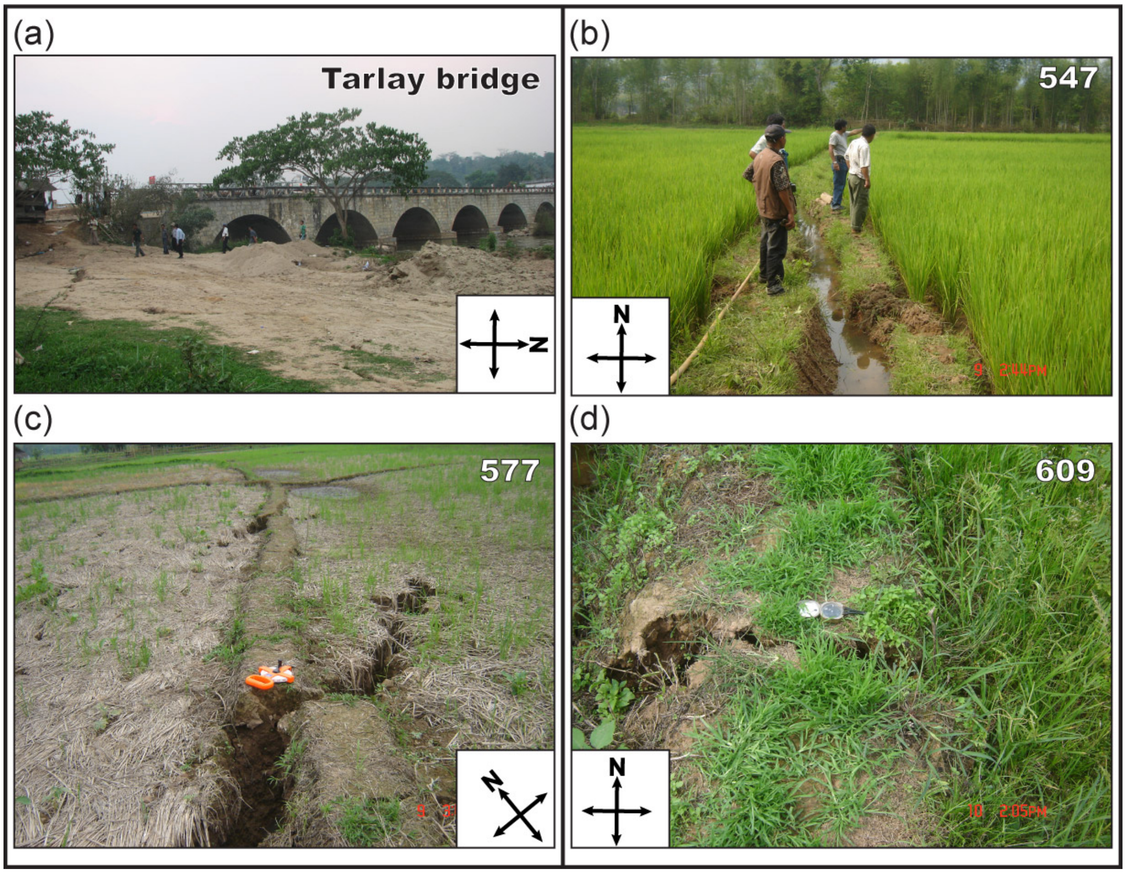

Figure 9. Photographs of left-lateral displacements near Tarlay that appear to be tectonic.
(a) Westward view of a faulted bridge embankment and the mostly undisturbed stone bridge across a river.
(b) 40-cm left-lateral offset on a narrow rupture crossing an irrigation channel and two paddy berms at Waypoint 547.
(c) Dual traces of the fault rupture offset a paddy field by 22 cm (in the foreground) and 15 cm (in the background) at Waypoint 577. The vertical displacement is a few cm at this location.
(d) 15-cm left-lateral offset of the paddy field boundary near Waypoint 609. The south side moved slightly down.

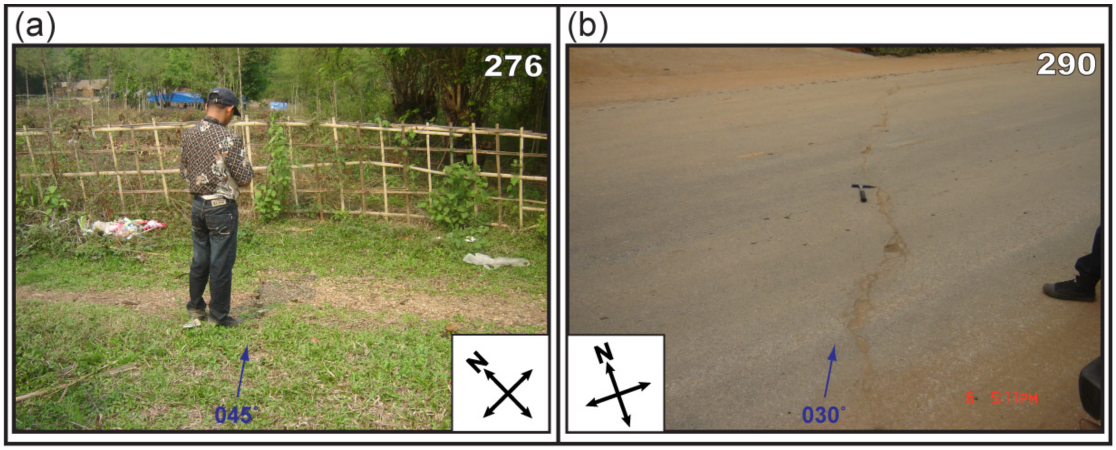

Figure 10. Photographs of ground cracks and fissures north of Tarlay.

(a) Ground fissure near the mountain front east of Tarlay, near Waypoint 276. The bamboo fence next to the fissure shows no horizontal displacement.

(b) Surface cracks across the paved road northwest of Tarlay, near Waypoint 290. The edge of the pavement does not clearly show horizontal displacement along the crack.

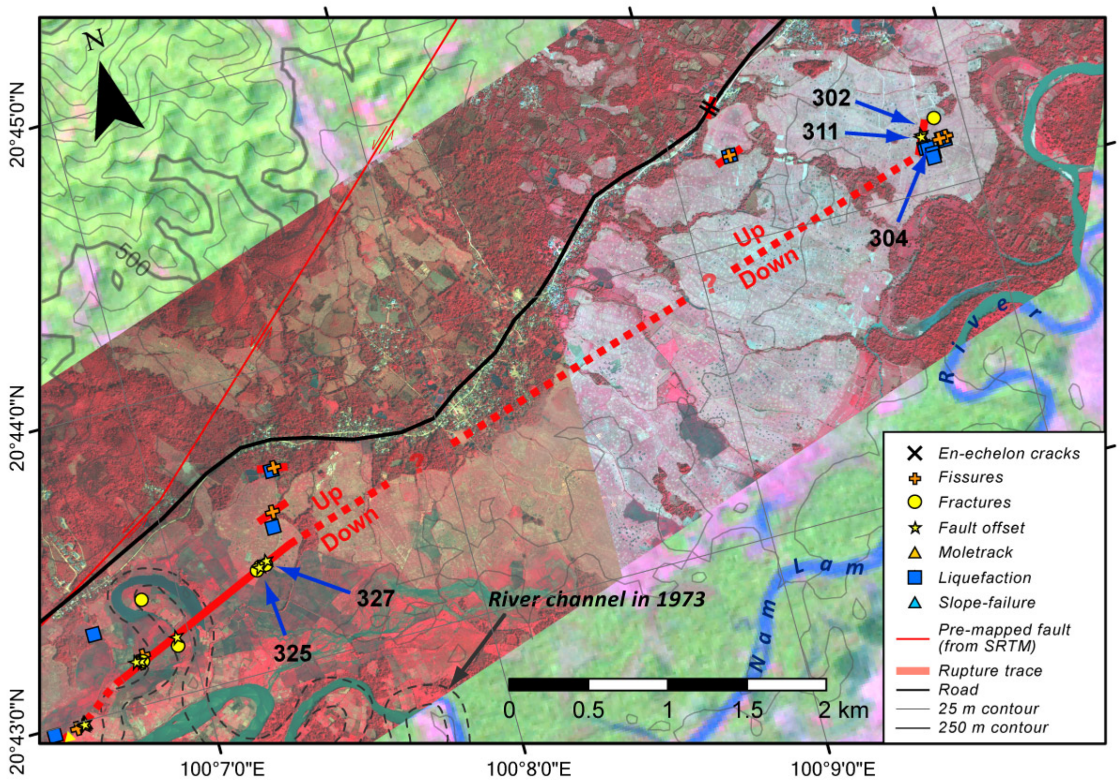

Figure 11. Map of the sites with horizontal offsets east of Tarlay.

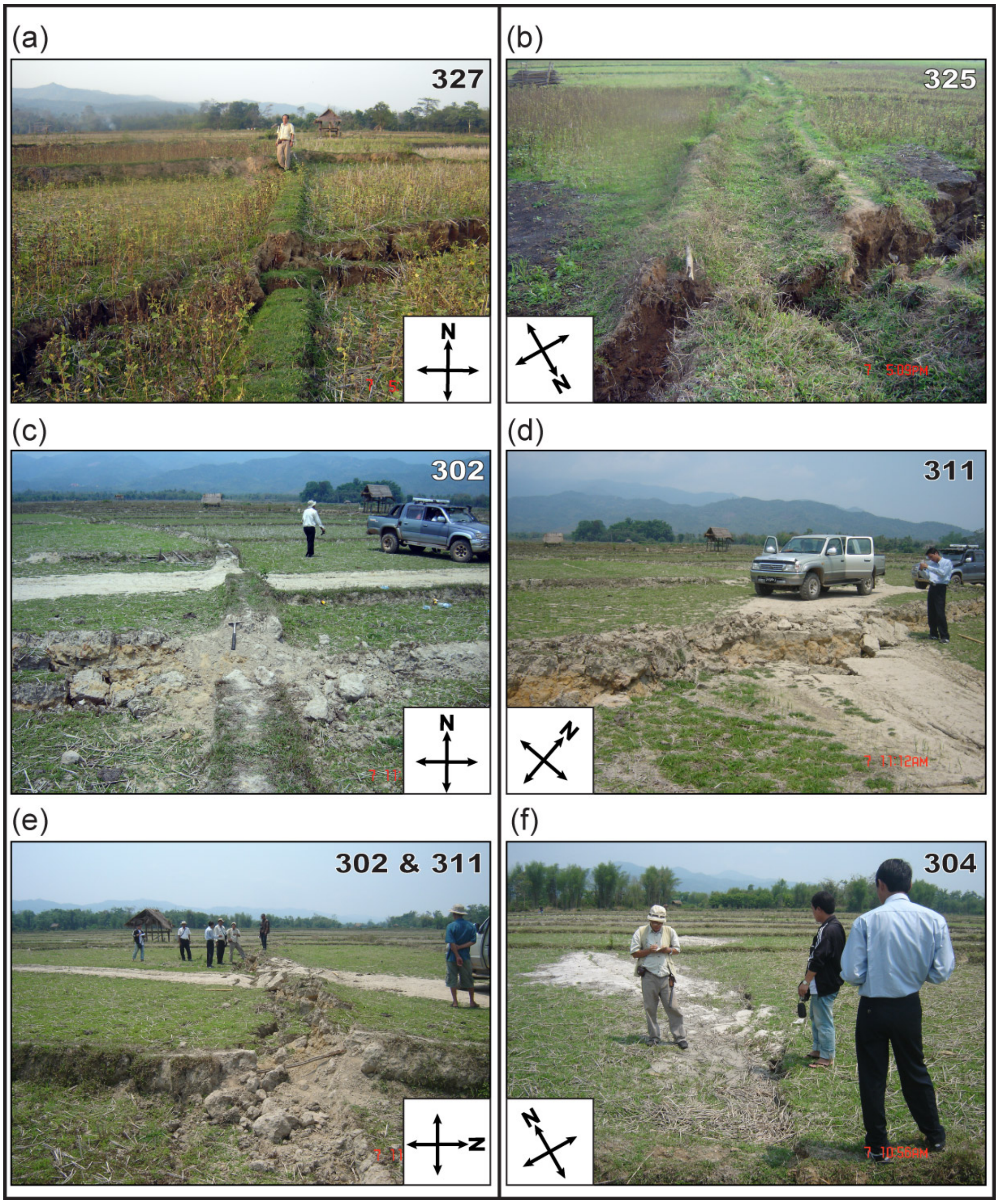

Figure 12. Photos of plausible tectonic offsets east of Tarlay.

(a) Left-lateral offset of 20 cm at Waypoint 327. The vertical displacement is 20 cm.
(b) Left-lateral offset is 30 cm at Waypoint 325. No vertical displacement.
(c) Right-lateral offset of 6 cm at Waypoint 302. The vertical displacement is approximately 15 cm.
(d) Purely dip-slip offset of 40 cm at Waypoint 311, close to Waypoint 302.
(e) A southwestward view of the surface rupture at Waypoints 302 and 311.
(f) A long fissure and accompanying sand blows at Waypoint 304, south of the fault rupture.

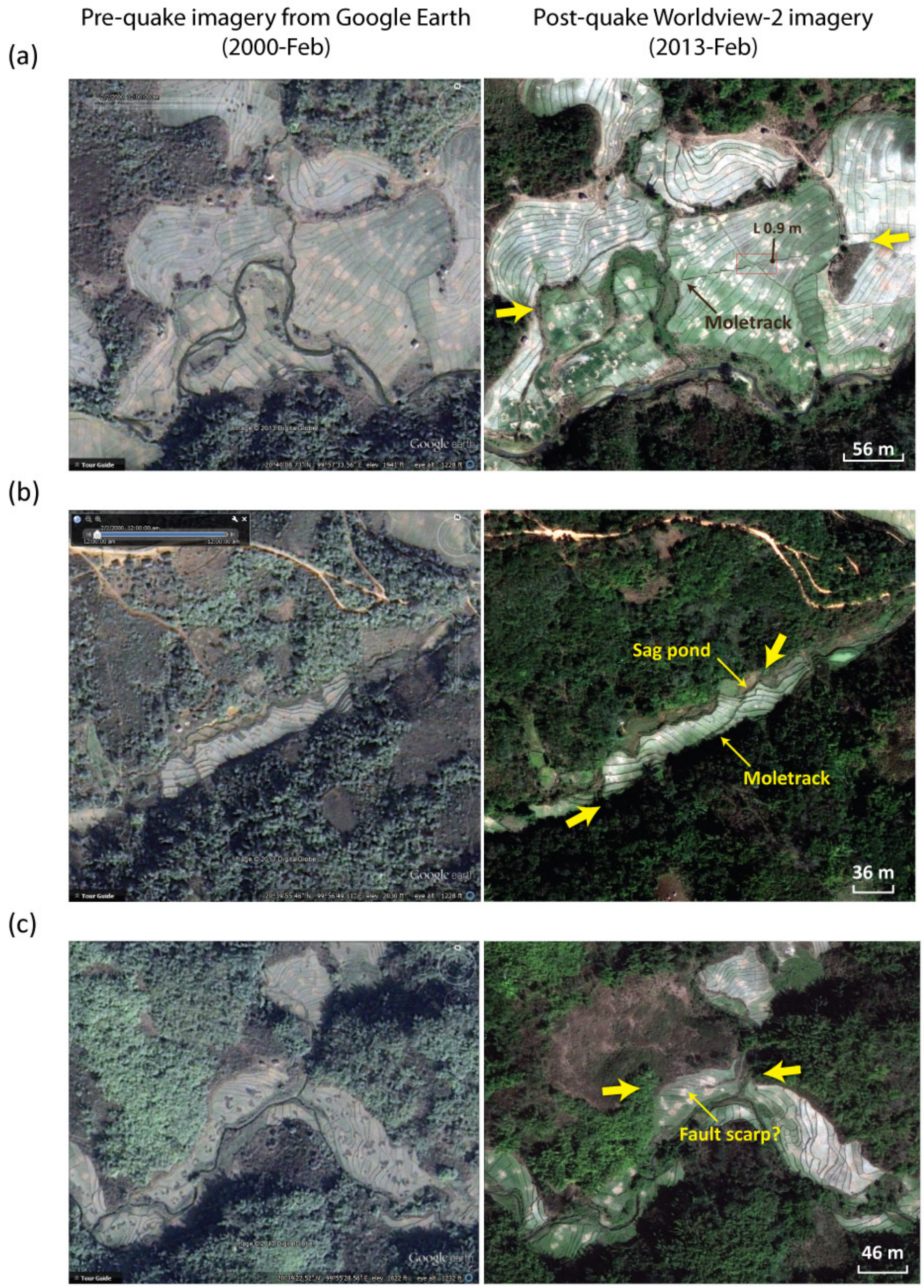

Figure 13. The pre-earthquake and post-earthquake HRS image west of the Kya Ku Ni site. (a) The preserved fault trace in the paddy fields about 1-km west of our last surveyed surface ruptures location, showing more than 0.9 m left-lateral displacement along the rupture. (b) The preserved fault trace and sag pond in the riverbed. See text for detail discussion. (c) The suspect preserved fault rupture in the river valley, about 6-km west of our last field surveyed location.

Table 1. Field measurements of the surface rupture of the 24 March 2011 Tarlay earthquake.

Waypoint	Date	Location (WGS 84)		Strike of feature	Offset (in cm)		Description
		LAT	LON		L-lateral offset	Vertical offset	
293	6-Apr-11	20.70992	100.09478	E-W	53	S	Offset of Tarlay bridge (eastern side)
302	7-Apr-11	20.73650	100.16414	20º	-6.36	15.24	Offset paddy field berm
311	7-Apr-11	20.73639	100.16408	25º		40	Offset dirt road and field
325	7-Apr-11	20.72244	100.12150	70º	30	S	Offset paddy field berm and dirt road
327	7-Apr-11	20.72272	100.12197	70º	20	20	offset field berm and fractures at fields
364	8-Apr-11	20.67292	99.97911	70º	12	S	Offset paddy field berm
368	8-Apr-11	20.67294	99.97917	70º	50		Offset paddy field berm
371	8-Apr-11	20.67294	99.97925	70º	82		Offset paddy field berm
373	8-Apr-11	20.67300	99.97939	70º	110		Offset paddy field berm and water channel
374	8-Apr-11	20.67306	99.97956	70º	125		Offset paddy field berm
403	8-Apr-11	20.67308	99.97967	70º	100		Offset paddy field berm
405	8-Apr-11	20.67311	99.97981	70º	110		Offset paddy field berm
407	8-Apr-11	20.67314	99.97992	70º	80		Offset paddy field berm
408	8-Apr-11	20.67317	99.98003	70º	90		Offset paddy field berm
409	8-Apr-11	20.67322	99.98011	70º	85		Offset paddy field berm
414	8-Apr-11	20.67333	99.98072	70º	52		Offset paddy field berm
416	8-Apr-11	20.67339	99.98100	70º	70		Offset paddy field berm and water channel
418	8-Apr-11	20.67342	99.98119	70º	120		Offset paddy field berm
420	8-Apr-11	20.67347	99.98139	70º	74		Offset paddy field berm
421	8-Apr-11	20.67350	99.98153	70º	47		Offset paddy field berm
425	8-Apr-11	20.67361	99.98186	70º	50		Offset paddy field berm
426	8-Apr-11	20.67364	99.98197	70º	75		Offset paddy field berm
427	8-Apr-11	20.67367	99.98208	70º	77		Offset paddy field berm, and moletrack
428	8-Apr-11	20.67369	99.98214	70º	55		Offset paddy field berm
429	8-Apr-11	20.67372	99.98231	70º	40		Offset paddy field berm
432	8-Apr-11	20.67389	99.98283	70º	100		Offset paddy field berm
434	8-Apr-11	20.67397	99.98311	70º	55		Offset paddy field berm
435	8-Apr-11	20.67397	99.98319	70º	72		Offset paddy field berm
436	8-Apr-11	20.67400	99.98333	70º	95		Offset paddy field berm

Table 1. Field measurements of the surface rupture of the 24 March 2011 Tarlay earthquake. (Continued)

Waypoint	Date	Location (WGS 84)		Strike of feature	Offset (in cm)		Description
		LAT	LON		L-lateral offset	Vertical offset	
438	8-Apr-11	20.67411	99.98367	70º	74		Offset paddy field berm
439	8-Apr-11	20.67411	99.98375	70º	60		Offset paddy field berm
444	8-Apr-11	20.67458	99.98511	70º	105		Offset paddy field berm
445	8-Apr-11	20.67458	99.98511	70º	105		Offset paddy field berm
446	8-Apr-11	20.67461	99.98519	70º	125		Offset paddy field berm
447	8-Apr-11	20.67464	99.98531	70º	100		Offset paddy field berm
449	8-Apr-11	20.67469	99.98542	70º	80		Offset paddy field berm
452	8-Apr-11	20.67481	99.98567	70º	110		Offset paddy field berm, and moletrack
453	8-Apr-11	20.67481	99.98569	70º	110		Offset paddy field berm, and moletrack
465	8-Apr-11	20.67544	99.98747	70º	45		Offset oblique paddy field berm
547	9-Apr-11	20.71117	100.09997	70º	40		Offset paddy field berm and water channel
564	9-Apr-11	20.71117	100.09997	70º	15		Offset paddy field berm
577	9-Apr-11	20.71644	100.10967	70º	22	S	Offset paddy field berm
578	9-Apr-11	20.71647	100.10972	70º	15		Offset paddy field berm
608	10-Apr-11	20.71983	100.11594	88º	15	SE	Offset paddy field berm
609	10-Apr-11	20.71983	100.11594	88º	15	SE	Offset paddy field berm
610	10-Apr-11	20.71944	100.11589	30º	-10	SE	Right-lateral offset of paddy field berm
613	10-Apr-11	20.71911	100.11372	30º	-13	SE	Right-lateral offset of paddy field berm
615	10-Apr-11	20.71903	100.11364	70º	36	S	Offset paddy field berm
617	10-Apr-11	20.71908	100.11333	30º	15		Disturbed field boundary